

1 **Molybdenum-Catalyzed Perchlorate Reduction: Robustness, Challenges, and Solutions**

2 Changxu Ren,^{1,§} Eric Y. Bi,^{1,2,§} Jinyu Gao,¹ and Jinyong Liu^{1,*}

3 ¹Department of Chemical and Environmental Engineering, University of California, Riverside, CA 92521, United
4 States.

5 ²Martin Luther King High School, Riverside, CA 92508, United States.

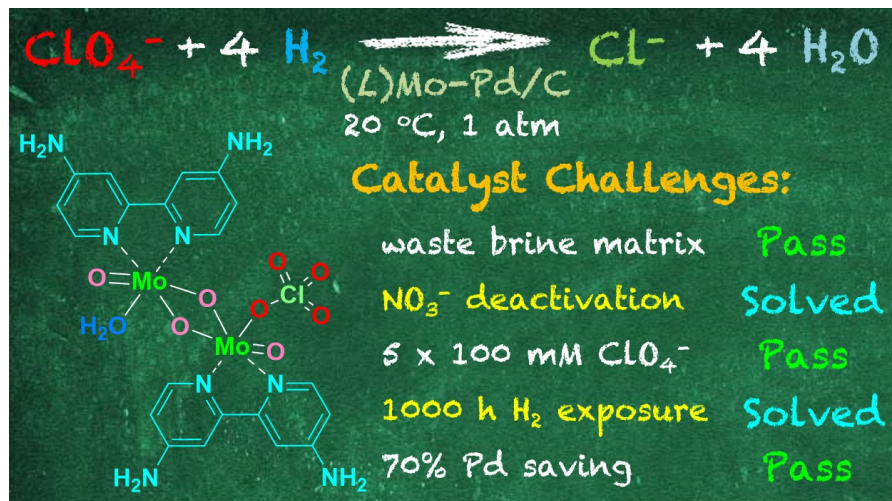
6 **ABSTRACT**

7 We have recently developed a highly active ligand-enabled (*L*)Mo–Pd/C catalyst (*L* = 4,4'-
8 diamino-2,2'-bipyridine) for aqueous perchlorate (ClO_4^-) reduction with 1 atm H_2 at room
9 temperature. This study reports on a series of satisfactory properties of this catalyst closely relevant
10 to ClO_4^- treatment in waste brines resulting from ion-exchange resin regeneration. In the presence
11 of concentrated salts and humic acid, the catalyst experienced limited inhibition but completed
12 ClO_4^- reduction in a few hours with an adjustable loading between 0.2 and 2 g/L. The catalyst was
13 not deactivated by the high oxidative stress from multiple spikes of 100 mM ClO_4^- . The challenge
14 of deactivation by nitrate was solved by pretreating the brine with In–Pd/Al₂O₃. The loss of activity
15 upon ligand hydrogenation was overcome by regenerating the Pd/C at pH 12. We also optimized
16 the catalyst formulation and saved 70% of Pd without sacrificing the activity. The substantially
17 enhanced performance and lowered adverse environmental impacts of (*L*)Mo–Pd/C make the
18 catalytic treatment competitive to microbial reactors for ClO_4^- reduction. We showcase the power
19 of coordination chemistry in environmental technology innovation and expect this catalyst to
20 promote the reuse of ClO_4^- -selective resins for sustainable water treatment.

21 **KEYWORDS**

22 palladium; brine; regeneration; deactivation; ion-exchange

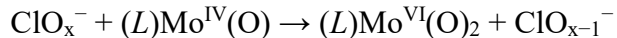
23 **TOC**



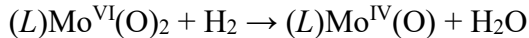
25 **INTRODUCTION**

26 The excess uptake of perchlorate (ClO_4^-) through contaminated water and food can disrupt
 27 thyroid hormone production, which is critical for the growth, development, metabolism, and
 28 mental function of humans.¹ In the United States, California² and Massachusetts³ set the maximum
 29 contamination level for ClO_4^- in drinking water at 6 and 2 $\mu\text{g/L}$, respectively. In China, the
 30 proposed 2021 revision of the National Standards for Drinking Water Quality included ClO_4^- at
 31 70 $\mu\text{g/L}$.⁴ With the improved understanding of ClO_4^- toxicity⁵ and the discovery of ClO_4^- on
 32 Mars,⁶ the remediation of ClO_4^- contamination is an imperative research topic for environmental
 33 engineering⁷⁻⁹ and space explorations.¹⁰⁻¹¹

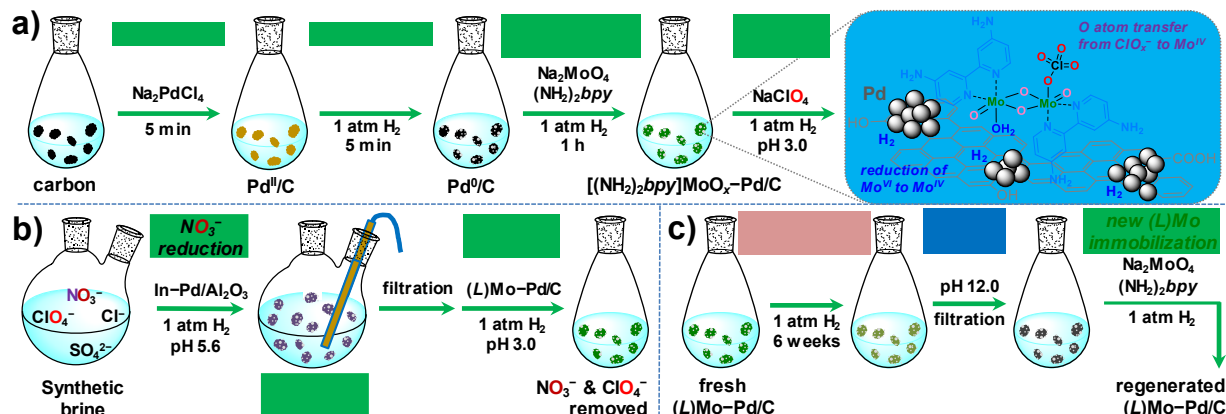
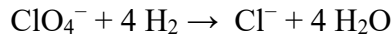
34 Although ion-exchange (IX) resins can readily remove ClO_4^- from water,¹² achieving a
 35 rapid reduction of enriched ClO_4^- has been a challenge for over two decades. Microbial reactors
 36 can take days to weeks to stabilize the function of ClO_4^- reduction,¹³⁻¹⁴ and most abiotic methods
 37 require harsh conditions and a large excess of reducing agents.¹⁵⁻¹⁹ The use of rhenium (Re) for
 38 ClO_4^- activation together with palladium (Pd) for H_2 activation (Re–Pd/C) realized rapid and
 39 complete reduction of ClO_4^- into Cl^- at ambient conditions.²⁰⁻²⁵ Recently, we have replaced Re
 40 with a highly reactive molybdenum (Mo) species, which was formed *in situ* from a common
 41 fertilizer, Na_2MoO_4 , and a common bipyridine ligand (*L*) (Figure 1).²⁶ In comparison to Re–Pd/C
 42 catalysts, the new (*L*)Mo–Pd/C shows even higher activity, does not involve specialized
 43 preparation procedures and is not deactivated by air exposure.²⁶ Spectroscopic evidence suggested
 44 a dimeric structure of the surface-immobilized Mo site, with each Mo coordinating with an *N,N*-
 45 bidentate ligand.²⁶ The coordination of Mo with the electron-rich ligand enables the rapid reaction
 46 with highly inert ClO_4^- via oxygen atom transfer to the reduced Mo^{IV} site:



47 The oxidized Mo^{VI} is then reduced back to Mo^{IV} by Pd-catalyzed hydrogenation:



48 The overall reaction is the complete and clean reduction of ClO_4^- :



53 **Figure 1.** Illustrated experimental procedures for (a) preparation of (*L*)Mo–Pd/C with adjustable Pd and
 54 Mo contents, (b) sequential reduction of NO_3^- by $\text{In-Pd/Al}_2\text{O}_3$ and ClO_4^- by (*L*)Mo–Pd/C, and
 55 (c) hydrogenation deactivation and regeneration of (*L*)Mo–Pd/C.

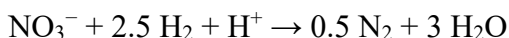
56 To promptly transfer the exciting invention into engineering solutions, herein we report on
57 systematic evaluation and improvement of the (L)Mo–Pd/C catalyst in terms of various
58 conventional and novel properties closely relevant to practical applications, including i)
59 performance in water matrices of concentrated salts and natural organics, ii) longevity in
60 challenging and continuous oxidative and reducing environments, and iii) cost-effectiveness
61 optimized through catalyst formulation. In particular, we provide viable solutions to catalyst
62 deactivation challenges. The results will guide the application of this catalyst and exemplify lab-
63 scale evaluations of new water treatment catalysts.

64 **MATERIALS AND METHODS**

65 **Chemicals and Materials.** $\text{Na}_2\text{MoO}_4 \cdot 2\text{H}_2\text{O}$ ($\geq 99\%$), Na_2PdCl_4 (98%), and humic acid
66 were purchased from Sigma–Aldrich. The ligand 4,4'-diamino-2,2'-bipyridine ($(\text{NH}_2)_2\text{bpy}$,
67 $>98\%$) was purchased from TCI America. NaClO_4 , NaCl , Na_2SO_4 , NaH_2PO_4 , NaNO_3 , NH_4Cl , and
68 NaOH in $\geq 99\%$ purities were purchased from Fisher Chemical. Ultrahigh purity (99.999%) H_2 gas
69 was purchased from Airgas. The standard 2 N sulfuric acid solution was purchase from Alfa Aesar.
70 All chemicals were used as received. Aqueous solutions were prepared with deionized (DI) water
71 (resistivity $>18.2 \text{ M}\Omega \text{ cm}$). The carbon support was purchased from Alfa Aesar (Norit GSX;
72 steam activated and acid-washed; surface area $1300 \text{ m}^2/\text{g}$) and used as received.

73 **Preparation and Use of (L)Mo–Pd/C Catalyst.** In this study, we prepared the catalyst
74 with various formulations from pristine activated carbon, Pd^{II} and Mo^{VI} precursors, and free ligand
75 (Figure 1a). The first step followed our previously developed *in situ* method to prepare Pd/C .²⁷
76 The amounts of carbon and Pd are adjustable based on the specific catalyst powder loading in
77 water (0.2–2.0 g/L) and the specific Pd content in the catalyst (0.1–5.0 wt%). In a 50-mL flask,
78 activated carbon powder was added to 50 mL of DI water. The flask was capped with a rubber
79 stopper, and the mixture was sonicated for 1 min. Under magnetic stirring, Na_2PdCl_4 solution was
80 added dropwise into the carbon suspension. Stirring for another 5 min was sufficient for Pd^{II}
81 immobilization onto carbon support. H_2 gas was supplied through a 16-gauge stainless steel needle.
82 Another needle was used as the gas outlet so that the H_2 pressure in the flask was maintained at 1
83 atm. The exposure to H_2 for 5 min was sufficient to reduce all Pd^{II} into Pd^0 nanoparticles.²⁷ The
84 resulting Pd/C catalyst could be either immediately added with Mo or filtered and dried under
85 vacuum for future use. In the second step, stock solutions of Na_2MoO_4 and $(\text{NH}_2)_2\text{bpy}$ were
86 sequentially added in the Pd/C suspension. The solution pH was adjusted to 3.0 using 2N H_2SO_4 .
87 The amount of Mo is adjustable for specific Mo content in the catalyst (0.5–5.0 wt%), whereas the
88 molar ratio of L:Mo was kept at 1:1. The following exposure to 1 atm H_2 for 1 h afforded the final
89 (L)Mo–Pd/C catalyst.²⁶ The addition of NaClO_4 (1–100 mM) initiated the catalytic reduction at
90 room temperature (20 °C). Aliquots were collected intermittently from the gas outlet needle and
91 immediately filtered by 0.22- μm cellulose acetate membrane to quench reactions.

92 **Perchlorate Reduction in the Synthetic Brine.** After (L)Mo–Pd/C was prepared, solid
93 salts were added to the catalyst suspension following the composition of a previously studied waste
94 brine (Table 1) collected from a Californian water treatment plant using a regenerable ion-
95 exchange system.²¹ Because the reduction of NO_3^- consumes H^+ :²¹



98 a 50-mL double-neck flask was used to monitor and maintain the solution pH during the reaction.
99 Both necks were capped with rubber stoppers, one of which accommodated a Fisherbrand accumet
100 gel-filled pencil-thin pH combination electrode (Figure 1b). The other stopper accommodated the
101 two stainless needles for H₂ supply and sampling. H₂SO₄ (0.1 M) was added through the sampling
102 needle to adjust the pH back to the working range for the catalyst (3.0 ± 0.1).

103 **Table 1. Composition of the Synthetic IX Regenerant Brine**

component ^a	concentration
chloride	0.9 M (32.3 g/L as Cl ⁻ , ~5 wt% NaCl)
perchlorate	1 mM (100 mg/L as ClO ₄ ⁻) ^b
nitrate	38 mM (2.36 g/L as NO ₃ ⁻)
sulfate	48 mM (4.70 g/L as SO ₄ ²⁻)
phosphate	0.22 mM (20.9 mg/L as PO ₄ ³⁻)

104 ^aNa⁺ was the only cation introduced with the above anionic species because K⁺, Ca²⁺, and Mg²⁺ (taking a
105 small portion of total cations in the real brine) did not significantly impact reaction kinetics.²⁴ Although
106 present in the real waste brine, carbonate was not added to the synthetic brine because it was fully removed
107 as CO₂ bubbles during pH adjustment to 3.0.²¹

108 ^bThe ClO₄⁻ concentration in the real brine was 0.02 mM (~2 mg L⁻¹ as ClO₄⁻) because the IX resin was not
109 perchlorate-selective. We increased the concentration to 1 mM for (i) ensuring the accuracy of ClO₄⁻
110 quantitation in the concentrated salt matrix, (ii) comparing the catalyst performance with most experiments
111 that used 1 mM ClO₄⁻ as the probe. The catalyst is capable of reducing as low as 0.01 mM (~1 mg/L) ClO₄⁻
112 by >99% (i.e., <10 µg/L in the treated water).²⁶

113 **Preparation and Use of In–Pd/Al₂O₃ Catalyst.** A 5 wt % Pd on γ-Al₂O₃ (Pd/Al₂O₃)
114 catalyst and InCl₃ (98%) were purchased from Sigma–Aldrich and used as received. The InCl₃
115 was dissolved in ethanol and added in Pd/Al₂O₃ via incipient wetness following a reported
116 method.²⁸ The solid was dried in air at 120 °C for 4 h and reduced with H₂ for 12 h. Then the
117 catalyst was collected and used at 2 g/L to reduce NO₃⁻ in the synthetic brine. Due to the scope of
118 this work, the preparation and formulation of In–Pd/Al₂O₃ were not further optimized. The pH
119 monitoring and adjustment during NO₃⁻ reduction (5.6±0.2) followed the same reactor
120 configuration as described above. After NO₃⁻ reduction was complete, In–Pd/Al₂O₃ was filtered
121 out, and the treated brine was added with 0.2 g/L of (L)Mo–Pd/C to reduce ClO₄⁻ (Figure 1b).

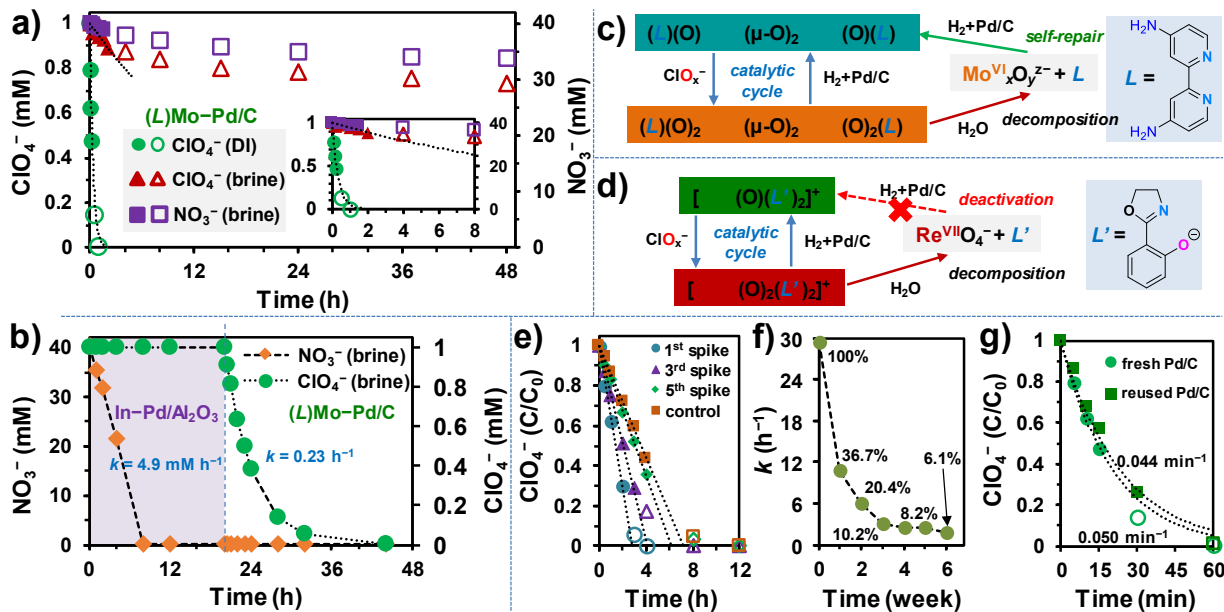
122 **Aqueous Sample Analysis.** The concentrations of ClO₄⁻ and NO₃⁻ were measured on an
123 ion chromatography (Dionex ICS-5000) with a conductivity detector and 25 µL sample loop. The
124 best separation of ClO₄⁻ from other anions was achieved by using a Dionex IonPac AS16 analytical
125 column at 30 °C with 1 mL/min of 65 mM KOH eluent. A Dionex IonPac AS 19 analytical column
126 was used to separate NO₃⁻. 20 mM KOH eluent was used to achieve the best separation. The
127 concentration of Mo in aqueous samples was analyzed by inductively coupled plasma–mass
128 spectrometry (ICP–MS, Agilent 7700). The concentration of the free (NH₂)₂bpy ligand was
129 quantified by high-performance liquid chromatography (Shimadzu Nexera XR) with a photodiode
130 array detector.

131 **Catalyst Collection and Elemental Analyses.** The catalyst powders, either freshly
132 prepared or used after reactions, were collected by vacuum filtration through a ceramic funnel
133 covered with Whatman qualitative filter paper. The filter paper was transferred into a 20-mL
134 scintillation vial and dried in an oven at 70 °C to remove moisture. The contents of Mo, Pd, C, H,
135 and N in the catalyst powders were determined by inductively coupled plasma–optical emission
136 spectrometry (ICP–OES, PerkinElmer Optima 8300) after microwave digestion in HNO₃–H₂O₂
137 (performed by the Microanalysis Laboratory at the University of Illinois at Urbana-Champaign).

138 **Regeneration of (L)Mo–Pd/C Catalyst.** This set of procedures is illustrated in Figure 1c.
 139 After the catalyst was deactivated by hydrogenation, the pH of the water suspension was adjusted
 140 to 12.0 with NaOH. The suspension was stirred for 10 min and filtered under vacuum. The
 141 collected solid was redispersed in DI water and added with new stock solutions of Na₂MoO₄ and
 142 (NH₂)₂bpy to regenerate the (L)Mo–Pd/C following the procedures described above.

143 **RESULTS AND DISCUSSION**

144 **Catalyst Performance for Brine Treatment.** We prioritize the evaluation of (L)Mo–Pd/C
 145 by assessing its performance in a practical scenario: ClO₄[−] reduction in a waste brine resulting
 146 from IX resin regeneration. Further assessment and development will be meaningful only if the
 147 catalyst can demonstrate satisfactory activity under challenging conditions. We prepared the
 148 synthetic brine containing all anion constituents in a previously studied brine (Table 1). Because
 149 early IX resins were not highly selective for ClO₄[−], the waste brines produced from resin
 150 regeneration typically contained sulfate, nitrate, and even phosphate at orders of magnitude higher
 151 concentrations than ClO₄[−].^{21,29–31} We added 1 mM ClO₄[−] in the synthetic brine (Table 1, footnote
 152 b). The ClO₄[−] reduction was conducted at the optimized pH of 3.0, and the complete conversion
 153 into Cl[−] has been confirmed.²⁶ Most abiotic ClO₄[−] reduction systems require H⁺ to enable oxygen
 154 atom transfer (OAT) in the aqueous phase.^{18,20–26,32–35}



155 **Figure 2.** Degradation of ClO₄[−] and NO₃[−] in the synthetic brine by (a) (L)Mo–Pd/C only and (b) sequential
 156 application of In–Pd/Al₂O₃ (2 g/L at pH 5.6) and (L)Mo–Pd/C; mechanistic schemes for (c) self-repair of
 157 (L)Mo–Pd/C and (d) deactivation of (L')₂Re–Pd/C caused by concentrated ClO₄[−]; (e) reduction of
 158 continuous spikes of 100 mM ClO₄[−] by 2 g/L of (L)Mo–Pd/C; (f) the decrease of ClO₄[−] reduction rate
 159 constants after continuous H₂ exposure; and (g) ClO₄[−] reduction by (L)Mo–Pd/C prepared from reused Pd/C
 160 after treatment at pH 12. Default reaction conditions: 0.2 g/L of (L)Mo–Pd/C (5 wt% Mo, 5 wt% Pd), pH
 161 3.0, 1 atm H₂, 20 °C. In panels a, e, and g, filled symbols were used to fit the 1st- or 0th-order model, whereas
 162 hollow ones were either not appropriate for fitting (i.e., C/C₀ < 0.2) or indicating the deviation from models.
 163

164 In comparison to the performance in deionized (DI) water (i.e., no concentrated brine
 165 constituents added), the synthetic brine matrix substantially retarded ClO₄[−] reduction (Figure 2a).

166 During the relatively fast reaction in the first 2 h, the barely fit first-order rate constant was only
 167 1.9% of that observed in DI water (Table 2 entry 5 versus 1). The gradually flattened kinetics
 168 suggested catalyst deactivation (i.e., loss of intrinsic activity). The simultaneous reduction of NO_3^-
 169 in the synthetic brine followed a similar trend (Figure 2a). To identify the deactivating species, we
 170 examined the effect of individual constituents on ClO_4^- reduction. In comparison to the DI water
 171 control, the addition of 80 mM H_2PO_4^- , 1 M SO_4^{2-} , and 1 M Cl^- lowered the rate constant by 37%,
 172 64%, and 86%, respectively (Table 2 entries 2–4 versus 1). However, these anions merely caused
 173 inhibition (i.e., decrease of reaction rate by reaction site competition) rather than deactivation. First,
 174 the ClO_4^- reduction followed the 1st-order kinetics well (Figure S1). The most inhibited catalyst in
 175 1 M NaCl still achieved >99.5% ClO_4^- reduction within 15 h (Figure S2). Second, recycling the
 176 catalyst from the previous use in 80 mM NaH_2PO_4 , 1 M Na_2SO_4 , or 1 M NaCl by filtration fully
 177 restored the activity (Figure S3). Although the catalyst was significantly inhibited by concentrated
 178 Cl^- , increasing the catalyst loading from 0.2 g/L to 2.0 g/L achieved >99.99% ClO_4^- reduction
 179 within 1 h (Figure S4). Notably, the activity was >13 times higher than that of the previously
 180 developed salt-resistant $\text{ReO}_x\text{--Pd/C}$ (Table 2 entry 4 versus 8 and 9).²¹

181 **Table 2. Rate Constants for ClO_4^- Reduction by Mo and Re Catalysts**

entry	other constituents in the solution	k ($\text{L h}^{-1} \text{g}_{\text{cat}}^{-1}$) ^a
[(NH ₂) ₂ bpy]MoO _x –Pd/C (5 wt% Mo, 5 wt% Pd)		
1	DI ^b	14.83 ± 0.37
2	80 mM NaH_2PO_4	12.26 ± 0.81
3	1 M Na_2SO_4	5.47 ± 0.23
4	1 M NaCl	2.19 ± 0.14
5	synthetic waste brine (see Table 1)	0.25 ± 0.04
6	synthetic waste brine without NO_3^-	2.12 ± 0.16
7	40 mM NH_4Cl	9.88 ± 0.39
$\text{ReO}_x\text{--Pd/C}$ (5 wt% Re, 5 wt% Pd)		
8	DI ^b	0.047 ± 0.003 ^c
9	1 M NaCl	0.16 ± 0.01 ^c
10	synthetic waste brine (see Table 1)	0.0079 ± 0.0003 ^c
11	synthetic waste brine without NO_3^-	0.18 ± 0.01 ^c

182 ^aApparent first-order rate constants (h^{-1}) for 1 mM ClO_4^-
 183 reduction (pH 3.0, 1 atm H_2 , 20 °C) normalized by the loading of
 184 catalyst powder in water ($\text{g}_{\text{cat}} \text{ L}^{-1}$) to facilitate cross-comparison.
 185 The loading of Mo- and Re-based catalysts used in experiments
 186 were 0.2 and 2.0 g/L, respectively.

187 ^bContaining ~1 mM H_2SO_4 (for pH adjustment to 3.0) and cations
 188 introduced with Na_2MoO_4 or KReO_4 precursor.

189 ^cData reported in Ref 21.

190 Hence, NO_3^- was the only remaining suspect for catalyst deactivation. We prepared a new
 191 synthetic brine that only excluded NO_3^- . In this brine, the ClO_4^- reduction profile resembled that
 192 in 1 M NaCl (Figure S2, Table 2 entry 4 versus 6), confirming that NO_3^- is responsible for catalyst
 193 deactivation. The slight inhibition in the presence of 40 mM NH_4Cl (assuming complete reduction
 194 of NO_3^- into NH_4^+)³⁶ is primarily attributed to Cl^- (Table 2 entry 7 versus 1 and 4) rather than
 195 NH_4^+ . In a separate experiment, we used (L)Mo–Pd/C to first treat 40 mM NO_3^- for 48 h. The
 196 water-rinsed catalyst only retained 11% of the original activity for ClO_4^- reduction (Figure S5).
 197 Because Pd-based catalysts integrating In, Cu, or Sn as the second metal have shown excellent
 198 NO_3^- reduction activities,³⁷ the severe deactivation of (L)Mo–Pd/C is attributed to the reaction

199 between NO_3^- (or intermediates such as NO_2^- , NO , and N_2O) with the $(L)\text{Mo}$ site rather than with
200 Pd . Inorganic chemistry studies using molecular Mo species for NO_3^- reduction have observed
201 inhibition by those nitrogen intermediates.³⁸⁻³⁹ Similar deactivation of the Re site has been
202 observed from the $\text{ReO}_x\text{-Pd/C}$ catalyst.²¹ While deeper mechanistic insights into the deactivation
203 phenomenon warrant further investigation, in this study, we prioritize the research effort as solving
204 this challenge by preventing NO_3^- from reacting with the Mo catalytic site.

205 **The Solution to Catalyst Deactivation by Nitrate.** We proposed a two-stage treatment to
206 protect $(L)\text{Mo-Pd/C}$ from reacting with NO_3^- (Figure 1b). In the first stage, NO_3^- in the synthetic
207 brine was reduced with a well-established $\text{In-Pd/Al}_2\text{O}_3$ catalyst.⁴⁰ Similar to the previous report,²¹
208 2 g/L of $\text{In-Pd/Al}_2\text{O}_3$ reduced $>99.98\%$ of the 38 mM of NO_3^- within 8 h (Figure 2b) with a $<30\%$
209 product selectivity toward NH_4^+ , whereas no ClO_4^- reduction was observed. Then we filtered out
210 $\text{In-Pd/Al}_2\text{O}_3$ and added 0.2 g/L of $(L)\text{Mo-Pd/C}$ into the nitrate-removed brine. As expected, the
211 reduction of 1 mM ClO_4^- proceeded rapidly and achieved 99.9% reduction within 24 h. The
212 $(L)\text{Mo-Pd/C}$ showed the highest ClO_4^- reduction activity in both DI water and brine among the
213 hydrogenation catalysts studied to date (Table S1).

214 **Catalyst Stability against Oxidative Stress.** After solving the nitrate deactivation
215 challenge, we evaluated the stability of $(L)\text{Mo-Pd/C}$ during the treatment of concentrated ClO_4^- .
216 The regeneration of ClO_4^- -selective resins can produce highly concentrated ClO_4^- up to 10 g/L
217 (~ 100 mM) within one bed volume of waste brine.^{12,15} Although ClO_4^- is highly inert, the ClO_x^-
218 intermediates are much more reactive with the $(L)\text{Mo}$ site,³⁴ where the ligand carries two strong
219 electron-donating $-\text{NH}_2$ groups. For Re-Pd/C catalysts prepared from presynthesized
220 $[\text{Re}^{\text{V}}(\text{O})(L')]^+$ (L' = various oxazoline-phenolate ligands) as the active site, concentrated ClO_x^-
221 could cause the accumulation of $[\text{Re}^{\text{VII}}(\text{O})_2(L')]^+$ and irreversible decomposition into ReO_4^- and
222 free L' (i.e., deactivation, Figure 2d).²⁴⁻²⁵ In contrast, the active $[(L)(\text{O})\text{Mo}^{\text{IV}}]_2(\mu\text{-O})_2$ site in
223 $(L)\text{Mo-Pd/C}$ is prepared *in situ* from inorganic molybdate and free $(\text{NH}_2)_2\text{bpy}$ ligand. If similar
224 hydrolysis of oxidized $[(L)(\text{O})\text{Mo}^{\text{VI}}]_2(\mu\text{-O})_2$ occurs, the products would be the starting materials,
225 allowing the active site to form again (i.e., self-repair, Figure 2c). To verify this hypothesis, we
226 challenged $(L)\text{Mo-Pd/C}$ with five spikes of 100 mM ClO_4^- . The reduction of the fifth ClO_4^- spike
227 was not slower than the control, where the fresh $(L)\text{Mo-Pd/C}$ reduced 100 mM ClO_4^- in the
228 presence of 400 mM Cl^- (Figure 2e and Table S2). Therefore, the gradual activity loss is attributed
229 to the accumulation of Cl^- from ClO_4^- reduction. After five spikes, each $(L)\text{Mo}$ site had undergone
230 1,920 redox turnovers without deactivation. Notably, the removal of 100 mM ClO_4^-
231 reached $>99.99\%$, more effective than the previously reported thermal treatment (92–98%).¹²

232 **Catalyst Longevity under Reducing Atmosphere.** It has been well documented that
233 pyridine structures are susceptible to Pd^0 -catalyzed hydrogenation, and those with electron-
234 donating substitutions (e.g., $-\text{NH}_2$) have the lowest reactivity.⁴¹⁻⁴² To evaluate the catalyst
235 longevity under extended hydrogenating conditions, we exposed the water suspension of
236 $(L)\text{Mo-Pd/C}$ to 1 atm H_2 atmosphere for up to 1000 h (6 weeks, Figure 1c). The rate constants for
237 ClO_4^- reduction decreased exponentially by 90% in the first three weeks (0.113 day^{-1} , Figure 2f
238 and Figure S6). The activity loss in weeks 4–6 was less pronounced and remained at 6% of the
239 original activity after 1000 h. We attribute the rapid activity decrease to the hydrogenation of
240 pyridyl rings in Mo-coordinated $(\text{NH}_2)_2\text{bpy}$. After that, the hydrogenation product still coordinated
241 with Mo and enabled ClO_4^- reduction to a limited extent. This interpretation is supported by the
242 limited ClO_4^- reduction activity using selected aliphatic diamine ligands and no activity without
243 using any organic ligand.²⁶

244 Elemental analyses of solid catalysts found that long-term exposure to H₂ caused roughly
 245 20% and 50% loss of Mo and N, respectively (Table 3 entry 4 versus 2). In comparison, the redox
 246 transformation during ClO₄⁻ reduction is not the cause for the leaching (Table 3 entry 3). In general,
 247 aliphatic amines have 5–6 units higher pKa values than pyridines (i.e., much more prone to be
 248 protonated). The hydrogenation of pyridyl structures might also eliminate the π-π stacking
 249 interaction with carbon support and thus enhance dissolution. The original (NH₂)₂bpy ligand was
 250 not detected in the water. In contrast, the Pd content did not significantly change in the solid, and
 251 ICP-MS analysis detected up to 0.01% of the total Pd dissolved in various water samples. Such
 252 stability is as expected because solid-state Pd⁰ can be readily maintained under H₂ atmosphere.²⁷

253 **Table 3. Elemental Analyses of Solid Catalysts (Unit: Weight Percentage, wt%)**

entry	Sample	Pd	Mo	Pd:Mo ^b	C	H	N
1	Pd/C without Mo ^a	3.86	0.01	-	83.61	1.14	0.52
2	fresh (L)Mo-Pd/C ^a	3.25	3.58	0.91:1	77.92	1.24	2.82
3	used (L)Mo-Pd/C after 1 mM ClO ₄ ⁻ treatment	3.09	3.23	0.96:1	77.30	1.24	2.74
4	after 6-week exposure under 1 atm H ₂	3.30	2.95	1.12:1	79.14	1.03	1.37
5	after regeneration at pH 12	3.53 ^c	0.03	-	83.41	1.29	2.04

254 ^aPd/C and (L)Mo-Pd/C had the nominal 5 wt% loadings for both Pd and Mo.

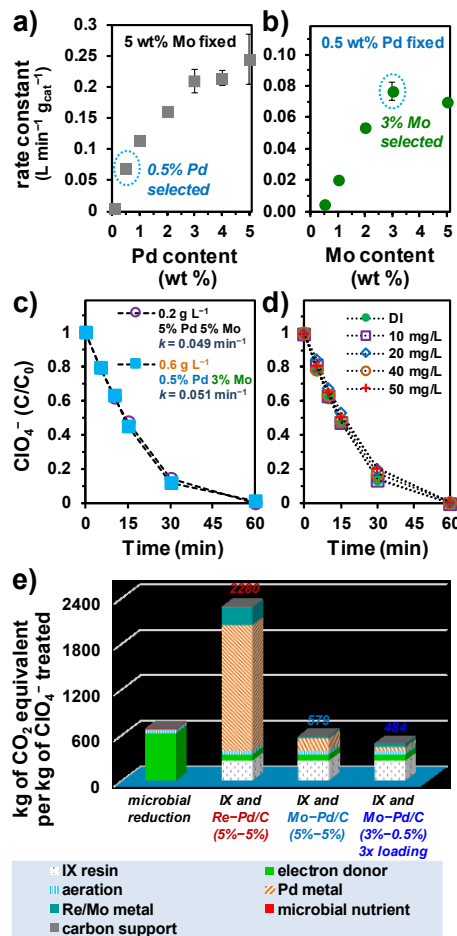
255 ^bBecause elemental analyses of solid samples always have deviations and can be significantly impacted by the addition
 256 of other constituents in the solid, the ratio between the two metals is a more meaningful indicator of metal leaching
 257 than the absolute weight percentage of each metal. Recall that Pd leaching is minimal under the H₂ atmosphere.²⁷

258 ^cFor the same reason as footnote b, this value is slightly lower than that in the original Pd/C (3.86% for Pd and 0.52
 259 for % N) because of the residual N (2.04%).

260 **Catalyst Regeneration after Ligand Hydrogenation.** The above findings suggest that the
 261 loss of the most precious component, Pd, is minimal. To restore the catalyst activity, we
 262 investigated the regeneration of Pd/C platform by removing Mo and hydrogenated ligand residues.
 263 Inspired by an early study on molybdate desorption from carbon,⁴³ we elevated the pH to 12 under
 264 air and achieved quantitative dissolution of Mo within 10 min (Figure S7). Elemental analysis of
 265 the solid confirmed the complete removal of Mo but incomplete removal of N-containing residues
 266 (Table 3 entry 5 versus 1). After adding fresh Na₂MoO₄ and (NH₂)₂bpy to the regenerated Pd/C
 267 (Figure 1c), the “refurbished” (L)Mo-Pd/C showed only slightly diminished activity (Figure 2g),
 268 probably due to the N-containing residues left on the carbon support. Hence, after several rounds
 269 of such regeneration, a complete recovery of Pd via chemical extractions⁴⁴⁻⁴⁶ could be necessary.

270 **Optimization of Catalyst Formulation.** To further reduce the use of Pd and maximize
 271 cost-effectiveness, we examined the effect of variable Pd and Mo contents on ClO₄⁻ reduction
 272 activity. Our recently developed method enables “instant” preparation of Pd/C with any metal
 273 content and significantly reduces the technical efforts for fine-tuning the metal contents.²⁷ With
 274 the Mo content fixed at 5 wt%, the decrease of Pd content by 90% (i.e., from 5 to 0.5 wt%) only
 275 lowered the rate constant by 71% (Figure 3a and Figure S8a), suggesting the feasibility of using
 276 less Pd to achieve the same catalytic activity at an increased loading of catalyst.²⁷ However, if the
 277 Mo content is kept at 5 wt%, the increased catalyst loading will involve more Mo and ligand.
 278 Interestingly, after the Pd content was lowered to 0.5 wt%, the initially optimized 5 wt% of Mo
 279 (using 5 wt% Pd/C)²⁶ became excessive, and 3 wt% was found to be the optimal content (Figure
 280 3b and Figure S8b). The tripled loading of 3 wt% Mo-0.5 wt% Pd/C exhibited the same rate of
 281 ClO₄⁻ reduction as the original 5 wt% Mo-5 wt% Pd/C (Figure 3c). Hence, the new formulation

282 involved a tripled amount of carbon and 80% more (*L*)Mo but saved 70% of Pd, the most expensive
 283 component.



284
 285 **Figure 3.** Optimization of (a) Pd and (b) Mo content in the (*L*)Mo–Pd/C catalyst, and the ClO_4^- reduction
 286 performance (c) with two catalyst formulations and (d) in the presence of 10–50 mg/L humic acid (0.2 g/L,
 287 5 wt% Mo and 5 wt% Pd). Common reaction conditions: 1 mM ClO_4^- , pH 3.0, 1 atm H_2 , and 20 °C. Panel
 288 e shows the comparison of “global warming” impacts by microbial reduction and sequential IX-catalysis
 289 treatment based on the data in a previous LCA study.⁴⁷

290 A life cycle assessment (LCA) study comparing microbial and catalytic (using ReO_x –Pd/C) reduction of ClO_4^- found that the mining and refining of Pd and Re contributed to the majority of
 291 adverse environmental impacts.⁴⁷ Because Re is a minor component in Mo minerals, we assume
 292 that the adverse impacts from Mo are not higher than from Re. The activity of (*L*)Mo–Pd/C is
 293 and 10-fold higher than ReO_x –Pd/C in DI water and NO_3^- -free synthetic brine, respectively (Table
 294 2). Furthermore, catalyst optimization has saved 70% Pd to achieve the same activity. Based on
 295 all of these advancements, the environmental impacts from Pd can be reduced by at least 970 and
 296 33 folds for use in DI water and brine, respectively. With the same LCA metrics and 33-fold
 297 decrease of Pd consumption, the new catalytic ClO_4^- reduction module using (*L*)Mo–Pd/C coupled
 298 with ion-exchange resin has become comparable to microbial reduction (Figure 3e and Text S1).

300 **Implications to Perchlorate Treatment.** The above results showcase a highly active,
 301 robust, and cost-effective heterogeneous catalyst for ClO_4^- reduction. Regarding practical

application, it is essential to highlight four technical points. First, the treatment of resin regeneration waste is separated from the drinking water treatment loop. Any concern of the non-neutral pH and minimal leaching of Mo and ligand in the treated brine can be further addressed if necessary. More importantly, cost-effective degradation of concentrated pollutants will advance drinking water treatment technologies by allowing sustainable reuse of ClO_4^- -selective IX resins instead of incineration.^{12,48-49} Highly selective resins do not require frequent regeneration; thus, a continuous operation for ClO_4^- reduction may not be needed, alleviating catalyst deactivation caused by ligand hydrogenation and allowing the use of a batch reactor configuration. In such cases, abiotic catalysts also have unique advantages over microbial reactors, which usually require continuous operation. The U.S. EPA has included Mo on the Third Unregulated Contaminant Monitoring Rule (UCMR-3) with the minimum reporting level of 1 $\mu\text{g/L}$ in drinking water.⁵⁰ If the treated brine is recycled for resin regeneration, further studies are warranted to evaluate the potential transfer of leached Mo from waste brine treatment to drinking water. Second, the use of H_2 gas for reductive pollutant degradation has been widely adopted in environmental engineering projects.⁵¹⁻⁵⁶ Third, inorganic sulfide, a potent Pd poison that may be present in the wastes, can be instantly oxidized into inert SO_4^{2-} using common oxidants⁵⁷ to avoid catalyst fouling. Fourth, although dissolved organics might not be significant constituents in the waste brine,²¹ our data show that 10–50 mg/L of humic acid did not inhibit the (L)Mo–Pd/C catalyst (Figure 3d). Although humic acid is a well-known inhibitor to Pd catalysts,³⁷ it appears that the $(\text{NH}_2)_2\text{bpy}$ -coordinated Mo sites are not sensitive to external ligands (e.g., the carboxylate groups in humic acid) and thus preserved the overall activity of (L)Mo–Pd/C. We will continue the study on the treatment of waste brines from the regeneration of perchlorate-selective resins. The brine has been reported to contain concentrated ClO_4^- (~100 mM) and $[\text{FeCl}_4]^-$ (from 1 M FeCl_3 and 4 M HCl).¹² Natural organic matters released from the resin are also expected to be abundant due to the long enrichment for six months. We will report unexpected case-specific challenges and technical solutions from pilot-scale testings of the (L)Mo–Pd/C catalyst used for the regeneration of perchlorate-selective resins.

Implications to Catalyst Development. The (L)Mo site is generated *in situ* via non-covalent Mo–N bonding and immobilized on carbon support via non-covalent interactions. The structure is also subject to decomposition upon dissolution²⁶ or significant pH adjustment from 3 to 12. However, under optimized conditions, the (L)Mo–Pd/C catalyst exhibits satisfactory performance in various parameters regarding practical applications, including unprecedentedly high activity for ClO_4^- reduction and resistance to oxidative stress. Moreover, the dynamic property of the (L)Mo complex also enables facile catalyst regeneration. Besides our continuous research efforts for Re-based catalysts,^{25,58-60} this study highlights the value of coordination metal complexes for environmental technology innovation aiming at practical engineering treatment.

ASSOCIATED CONTENT

Supporting Information

The Supporting Information is available free of charge on the ACS Publications website at DOI: 10.1021/acsestengg.XXXXXXX.

Kinetic profiles of perchlorate and nitrate reduction under various conditions; the comparison with Re-based catalysts; details for the estimation of environmental impact values.

AUTHOR INFORMATION

345 [§]These authors contributed equally.

346 **Corresponding Author**

347 *(J.L.) E-mail: jylu@engr.ucr.edu; jinyong.liu101@gmail.com.

348 **Notes**

349 The authors declare no competing financial interest.

350 **ACKNOWLEDGMENTS**

351 Financial support was provided by the National Science Foundation (Award No. CBET-1932942).

352 **REFERENCES**

- 353 1. Greer, M. A.; Goodman, G.; Pleus, R. C.; Greer, S. E. Health effects assessment for environmental
354 perchlorate contamination: The dose response for inhibition of thyroidal radioiodine uptake in humans.
355 *Environ. Health Perspect.* **2002**, *110*, 927-937.
- 356 2. California State Water Resources Control Board: Perchlorate in Drinking Water.
357 https://www.waterboards.ca.gov/drinking_water/certlic/drinkingwater/Perchlorate.html (accessed 2021-
358 09-29).
- 359 3. Massachusetts Department of Environmental Protection: Perchlorate Background Information and
360 Standards. <https://www.mass.gov/lists/perchlorate-background-information-and-standards#perchlorate---final-standards-> (accessed 2021-09-29).
- 361 4. National Standard of the People's Republic of China: GB 5749-XXXX (to replace GB 5749-2006)
362 Standards for Drinking Water Quality. **2021**,
363 http://www.cuwa.org.cn/Uploads/file/20210715/20210715225950_71443.pdf (accessed 2021-09-29).
- 364 5. Llorente-Esteban, A.; Manville, R. W.; Reyna-Neyra, A.; Abbott, G. W.; Amzel, L. M.; Carrasco,
365 N. Allosteric regulation of mammalian Na^+/I^- symporter activity by perchlorate. *Nat. Struct. Mol. Biol.*
366 **2020**, *27*, 533-539.
- 367 6. Hecht, M.; Kounaves, S.; Quinn, R.; West, S.; Young, S.; Ming, D.; Catling, D.; Clark, B.; Boynton,
368 W. V.; Hoffman, J. Detection of perchlorate and the soluble chemistry of martian soil at the Phoenix lander
369 site. *Science* **2009**, *325*, 64-67.
- 370 7. Hatzinger, P. B. Perchlorate biodegradation for water treatment. *Environ. Sci. Technol.* **2005**, *39*,
371 239A-247A.
- 372 8. Khera, R.; Ransom, P.; Guttridge, M.; Speth, T. F. Estimating costs for nitrate and perchlorate
373 treatment for small drinking water systems. *AWWA Water Sci.* **2021**, *3*, e1224.
- 374 9. United States Environmental Protection Agency: Perchlorate in Drinking Water.
375 <https://www.epa.gov/sdwa/perchlorate-drinking-water> (accessed 2021-08-01).
- 376 10. Davila, A. F.; Willson, D.; Coates, J. D.; McKay, C. P. Perchlorate on Mars: A chemical hazard
377 and a resource for humans. *Int. J. Astrobiol.* **2013**, *12*, 321-325..
- 378 11. Schuttlefield, J. D.; Sambur, J. B.; Gelwicks, M.; Eggleston, C. M.; Parkinson, B. Photooxidation
379 of chloride by oxide minerals: Implications for perchlorate on Mars. *J. Am. Chem. Soc.* **2011**, *133*, 17521-
380 17523.
- 381 12. Gu, B.; Brown, G. M.; Chiang, C.-C. Treatment of perchlorate-contaminated groundwater using
382 highly selective, regenerable ion-exchange technologies. *Environ. Sci. Technol.* **2007**, *41*, 6277-6282.
- 383 13. Coates, J. D.; Achenbach, L. A. Microbial perchlorate reduction: Rocket-fuelled metabolism. *Nat.*
384 *Rev. Microbiol.* **2004**, *2*, 569-580.

386 14. Lai, C.-Y.; Wu, M.; Lu, X.; Wang, Y.; Yuan, Z.; Guo, J. Microbial perchlorate reduction driven by
387 ethane and propane. *Environ. Sci. Technol.* **2021**, *55*, 2006-2015.

388 15. Gu, B.; Dong, W.; Brown, G. M.; Cole, D. R. Complete degradation of perchlorate in ferric chloride
389 and hydrochloric acid under controlled temperature and pressure. *Environ. Sci. Technol.* **2003**, *37*, 2291-
390 2295.

391 16. Cao, J.; Elliott, D.; Zhang, W.-x. Perchlorate reduction by nanoscale iron particles. *J. Nanopart. Res.* **2005**, *7*, 499-506.

393 17. Xiong, Z.; Zhao, D.; Pan, G. Rapid and complete destruction of perchlorate in water and ion-
394 exchange brine using stabilized zero-valent iron nanoparticles. *Water Res.* **2007**, *41*, 3497-3505.

395 18. Wang, C.; Huang, Z.; Lippincott, L.; Meng, X. Rapid Ti(III) reduction of perchlorate in the
396 presence of β -alanine: Kinetics, pH effect, complex formation, and β -alanine effect. *J. Hazard. Mater.* **2010**,
397 *175*, 159-164.

398 19. Hori, H.; Sakamoto, T.; Tanabe, T.; Kasuya, M.; Chino, A.; Wu, Q.; Kannan, K. Metal-induced
399 decomposition of perchlorate in pressurized hot water. *Chemosphere* **2012**, *89*, 737-742.

400 20. Hurley, K. D.; Shapley, J. R. Efficient heterogeneous catalytic reduction of perchlorate in water.
401 *Environ. Sci. Technol.* **2007**, *41*, 2044-2049.

402 21. Liu, J.; Choe, J. K.; Sasnow, Z.; Werth, C. J.; Strathmann, T. J. Application of a Re-Pd bimetallic
403 catalyst for treatment of perchlorate in waste ion-exchange regenerant brine. *Water Res.* **2013**, *47*, 91-101.

404 22. Hurley, K. D.; Zhang, Y.; Shapley, J. R. Ligand-enhanced reduction of perchlorate in water with
405 heterogeneous Re-Pd/C catalysts. *J. Am. Chem. Soc.* **2009**, *131*, 14172-14173.

406 23. Liu, J.; Choe, J. K.; Wang, Y.; Shapley, J. R.; Werth, C. J.; Strathmann, T. J. Bioinspired complex-
407 nanoparticle hybrid catalyst system for aqueous perchlorate reduction: Rhenium speciation and its influence
408 on catalyst activity. *ACS Catal.* **2015**, *5*, 511-522.

409 24. Liu, J.; Chen, X.; Wang, Y.; Strathmann, T. J.; Werth, C. J. Mechanism and mitigation of the
410 decomposition of an oxorhenium complex-based heterogeneous catalyst for perchlorate reduction in water.
411 *Environ. Sci. Technol.* **2015**, *49*, 12932-12940.

412 25. Ren, C.; Liu, J. Bioinspired catalytic reduction of aqueous perchlorate by one single-metal site with
413 high stability against oxidative deactivation. *ACS Catal.* **2021**, *11*, 6715-6725.

414 26. Ren, C.; Yang, P.; Sun, J.; Bi, E. Y.; Gao, J.; Palmer, J.; Zhu, M.; Wu, Y.; Liu, J. A bioinspired
415 molybdenum catalyst for aqueous perchlorate reduction. *J. Am. Chem. Soc.* **2021**, *143*, 7891-7896.

416 27. Gao, J.; Ren, C.; Huo, X.; Ji, R.; Wen, X.; Guo, J.; Liu, J. Supported palladium catalysts: A facile
417 preparation method and implications to reductive catalysis technology for water treatment. *ACS ES&T Eng.*
418 **2021**, *1*, 562-570.

419 28. Chaplin, B. P.; Shapley, J. R.; Werth, C. J. Regeneration of sulfur-fouled bimetallic Pd-based
420 catalysts. *Environ. Sci. Technol.* **2007**, *41*, 5491-5497.

421 29. Batista, J. R.; McGarvey, F. X.; Vieira, A. R. The removal of perchlorate from waters using ion-
422 exchange resins. In *Perchlorate in the Environment*; Springer, 2000; pp 135-145.

423 30. Gingras, T. M.; Batista, J. R. Biological reduction of perchlorate in ion exchange regenerant
424 solutions containing high salinity and ammonium levels. *J. Environ. Monit.* **2002**, *4*, 96-101.

425 31. Lehman, S. G.; Badruzzaman, M.; Adham, S.; Roberts, D. J.; Clifford, D. A. Perchlorate and nitrate
426 treatment by ion exchange integrated with biological brine treatment. *Water Res.* **2008**, *42*, 969-976.

427 32. Abu-Omar, M. M.; Espenson, J. H. Facile abstraction of successive oxygen atoms from perchlorate
428 ions by methylrhenium dioxide. *Inorg. Chem.* **1995**, *34*, 6239-6240.

429 33. Rechnitz, G. A.; Laitinen, H. A study of the molybdenum catalyzed reduction of perchlorate. *Anal.*
430 *Chem.* **1961**, *33*, 1473-1477.

431 34. Ren, C.; Yang, P.; Gao, J.; Huo, X.; Min, X.; Bi, E. Y.; Liu, Y.; Wang, Y.; Zhu, M.; Liu, J. Catalytic
432 reduction of aqueous chlorate with MoO_x immobilized on Pd/C. *ACS Catal.* **2020**, *10*, 8201-8211.

433 35. Liu, B. Y.; Wagner, P. A.; Earley, J. E. Reduction of perchlorate ion by (N-(hydroxyethyl)
434 ethylenediaminetriacetato) aquatitanium(III). *Inorg. Chem.* **1984**, *23*, 3418-3420.

435 36. Chen, X.; Huo, X.; Liu, J.; Wang, Y.; Werth, C. J.; Strathmann, T. J. Exploring beyond palladium:
436 Catalytic reduction of aqueous oxyanion pollutants with alternative platinum group metals and new
437 mechanistic implications. *Chem. Eng. J.* **2017**, *313*, 745-752.

438 37. Chaplin, B. P.; Reinhard, M.; Schneider, W. F.; Schüth, C.; Shapley, J. R.; Strathmann, T. J.; Werth,
439 C. J. Critical review of Pd-based catalytic treatment of priority contaminants in water. *Environ. Sci. Technol.*
440 **2012**, *46*, 3655-3670.

441 38. Majumdar, A.; Pal, K.; Sarkar, S., Selectivity of thiolate ligand and preference of substrate in model
442 reactions of dissimilatory nitrate reductase. *Inorg. Chem.* **2008**, *47*, 3393-3401.

443 39. Ehweiner, M. A.; Wiedemaier, F.; Belaj, F.; Mösch-Zanetti, N. C., Oxygen Atom Transfer
444 Reactivity of Molybdenum (VI) Complexes Employing Pyrimidine-and Pyridine-2-thiolate Ligands. *Inorg.*
445 *Chem.* **2020**, *59*, 14577-14593.

446 40. Prütse, U.; Vorlop, K.-D. Supported bimetallic palladium catalysts for water-phase nitrate
447 reduction. *J. Mol. Catal. A Chem.* **2001**, *173*, 313-328.

448 41. Cui, Y.; Kwok, S.; Bucholtz, A.; Davis, B.; Whitney, R. A.; Jessop, P. G. The effect of substitution
449 on the utility of piperidines and octahydroindoles for reversible hydrogen storage. *New J. Chem.* **2008**, *32*,
450 1027-1037.

451 42. Irfan, M.; Petricci, E.; Glasnov, T. N.; Taddei, M.; Kappe, C. O. Continuous flow hydrogenation
452 of functionalized pyridines. *Eur. J. Org. Chem.* **2009**, *2009*, 1327-1334.

453 43. Namasivayam, C.; Sangeetha, D. Removal of molybdate from water by adsorption onto ZnCl_2
454 activated coir pith carbon. *Bioresour. Technol.* **2006**, *97*, 1194-1200.

455 44. Fotouhi-Far, F.; Bashiri, H.; Hamadanian, M.; Keshavarz, M. H. A new approach for the leaching
456 of palladium from spent Pd/C catalyst in $\text{HCl}-\text{H}_2\text{O}_2$ system. *Prot. Met. Phys. Chem. Surf.* **2021**, *57*, 297-
457 305.

458 45. Fontana, D.; Pietrantonio, M.; Pucciarmati, S.; Torelli, G. N.; Bonomi, C.; Masi, F. Palladium
459 recovery from monolithic ceramic capacitors by leaching, solvent extraction and reduction. *J. Mater. Cycles*
460 *Waste Manag.* **2018**, *20*, 1199-1206.

461 46. Nogueira, C. A.; Paiva, A. P.; Costa, M. C.; da Costa, A. M. R. Leaching efficiency and kinetics of
462 the recovery of palladium and rhodium from a spent auto-catalyst in HCl/CuCl_2 media. *Environ. Technol.*
463 **2019**, *41*, 2293-2304.

464 47. Choe, J. K.; Mehnert, M. H.; Guest, J. S.; Strathmann, T. J.; Werth, C. J. Comparative assessment
465 of the environmental sustainability of existing and emerging perchlorate treatment technologies for drinking
466 water. *Environ. Sci. Technol.* **2013**, *47*, 4644-4652.

467 48. Sharbatmaleki, M.; Batista, J. R. Multi-cycle bioregeneration of spent perchlorate-containing
468 macroporous selective anion-exchange resin. *Water Res.* **2012**, *46*, 21-32.

469 49. Faccini, J.; Ebrahimi, S.; Roberts, D. J. Regeneration of a perchlorate-exhausted highly selective
470 ion exchange resin: Kinetics study of adsorption and desorption processes. *Sep. Purif. Technol.* **2016**, *158*,
471 266-274.

472 50. U.S. Environmental Protection Agency. Revisions to the unregulated contaminant monitoring
473 regulation (UCMR 3) for public water systems. *Fed. Regist.* **2012**, *77*, 26072-26101.

474 51. Zhou, D.; Luo, Y.-H.; Zheng, C.-W.; Long, M.; Long, X.; Bi, Y.; Zheng, X.; Zhou, C.; Rittmann,
475 B. E. H₂-Based membrane catalyst-film reactor (H₂-MCfR) loaded with palladium for removing oxidized
476 contaminants in water. *Environ. Sci. Technol.* **2021**, *55*, 7082-7093.

477 52. Luo, Y.-H.; Long, X.; Wang, B.; Zhou, C.; Tang, Y.; Krajmalnik-Brown, R.; Rittmann, B. E. A
478 synergistic platform for continuous co-removal of 1,1,1-trichloroethane, trichloroethene, and 1,4-dioxane
479 via catalytic dechlorination followed by biodegradation. *Environ. Sci. Technol.* **2021**, *55*, 6363-6372.

480 53. Zhao, H.-P.; Ontiveros-Valencia, A.; Tang, Y.; Kim, B. O.; Ilhan, Z. E.; Krajmalnik-Brown, R.;
481 Rittmann, B. Using a two-stage hydrogen-based membrane biofilm reactor (MBfR) to achieve complete
482 perchlorate reduction in the presence of nitrate and sulfate. *Environ. Sci. Technol.* **2013**, *47*, 1565-1572.

483 54. McNab, W. W.; Ruiz, R.; Reinhard, M. In-situ destruction of chlorinated hydrocarbons in
484 groundwater using catalytic reductive dehalogenation in a reactive well: Testing and operational
485 experiences. *Environ. Sci. Technol.* **2000**, *34*, 149-153.

486 55. Schüth, C.; Kummer, N.-A.; Weidenthaler, C.; Schad, H. Field application of a tailored catalyst for
487 hydrodechlorinating chlorinated hydrocarbon contaminants in groundwater. *Appl. Catal. B: Environ.* **2004**,
488 *52*, 197-203.

489 56. Davie, M. G.; Cheng, H.; Hopkins, G. D.; Lebron, C. A.; Reinhard, M. Implementing
490 heterogeneous catalytic dechlorination technology for remediating TCE-contaminated groundwater.
491 *Environ. Sci. Technol.* **2008**, *42*, 8908-8915.

492 57. Tomar, M.; Abdullah, T. H. Evaluation of chemicals to control the generation of malodorous
493 hydrogen sulfide in waste water. *Water Res.* **1994**, *28*, 2545-2552.

494 58. Liu, J.; Wu, D.; Su, X.; Han, M.; Kimura, S. Y.; Gray, D. L.; Shapley, J. R.; Abu-Omar, M. M.;
495 Werth, C. J.; Strathmann, T. J. Configuration control in the synthesis of homo- and heteroleptic bis
496 (oxazolinylphenolato/thiazolinylphenolato) chelate ligand complexes of oxorhenium(V): Isomer effect on
497 ancillary ligand exchange dynamics and implications for perchlorate reduction catalysis. *Inorg. Chem.* **2016**,
498 *55*, 2597-2611.

499 59. Liu, J.; Han, M.; Wu, D.; Chen, X.; Choe, J. K.; Werth, C. J.; Strathmann, T. J., A new bioinspired
500 perchlorate reduction catalyst with significantly enhanced stability via rational tuning of rhenium
501 coordination chemistry and heterogeneous reaction pathway. *Environ. Sci. Technol.* **2016**, *50*, 5874-5881.

502 60. Liu, J.; Su, X.; Han, M.; Wu, D.; Gray, D. L.; Shapley, J. R.; Werth, C. J.; Strathmann, T. J. Ligand
503 design for isomer-selective oxorhenium(V) complex synthesis. *Inorg. Chem.* **2017**, *56*, 1757-1769.

504